Leader-Follower of Quadrotor Micro Aerial Vehicle

Dwi Pebrianti[1], Yee Woon Chun[2], Yong Hooi Hao[3], Goh Ming Qian[1], Mahfuzah Mustafa[1],
Rosdiyana Samad[1] and Luhur Bayuaji[4]

[1]*Faculty of Electrical & Electronics Engineering, Universiti Malaysia Pahang, 26600, Pahang, Malaysia.*
[2]*Test Department, Texas Instrument Malaysia, Ampang/Ulu Klang Free Trade Zone, 54200, Kuala Lumpur, Malaysia.*
[3]*Electrical & Instrument Department, CNI Engineering Construction Sdn. Bhd., 81600, Johor, Malaysia.*
[4]*Faculty of Computer Science & Software Engineering, Universiti Malaysia Pahang, 26300, Pahang, Malaysia.*
dwipebrianti@ump.edu.my

Abstract—**A Micro Aerial Vehicle (MAV) is known as a drone or in a bigger size is called Unmanned Aerial Vehicle (UAV). Quadrotors are leading edge of a huge development in military and civilian such as disaster search and rescue, surveillance, aerial mapping and others. However, those applications limits by the payload delivered and long execution time. Hence, this study focuses on Leader-Follower approach of Quadrotor MAV. The study covers the development of quadrotor platform, modelling, controller design and leader-follower implementation. As the preliminary study, an Android phone is used as a leader which is used to provide the desired position and orientation to the follower quadrotor. The follower will be an autonomous quadrotor. Proportional Integral Derivative (PID) controller for the position and attitude control are first designed and tested via simulation. Then, a real flight implementation is conducted. The result shows that the follower can follow the leader on a circular path and straight line path. The settling time for X, Y and Z position of the follower is 10.22, 10.90 and 19.45 seconds, respectively. Additionally, the overshoot percentage for X, Y and Z position are 7%, 0% and 0%, respectively.**

Index Terms—**Leader Follower; Micro Aerial Vehicle; Position Control; PID Controller; Quadrotor**

I. INTRODUCTION

With the ever-changing nature of technology, the study of Unmanned Aerial Vehicles (UAVs) has become an inevitable trend. Recently, a growing number of researchers in UAVs have prominence the popularity and attention. UAV or Unmanned Aircraft System (UAS) is also well-known as a drone. UAV is a pilotless aircraft which means that the aircraft flies without the existing of a human pilot aboard. The flight of UAVs may operate with various degrees of autonomy, such as control remotely by a human operator, fully or intermittently autonomously by onboard computers. UAVs were developed or implemented into civil applications that are dirty, dangerous and dull at the beginning. In other words, it was invented to execute some tasks that touch upon hazard or risk for the pilot of manned aircraft. However, UAVs have been further developed into other potential scopes such as disaster rescue, disease detection, military, security, spy, mapping, forest fire detection, contamination measurement, and videography, etc.

Recently, application of formation control of UAVs has attracted much attention and has been arranged in fields including surveillance or exploration within some region, military, and civilian like search and rescue missions. In formation control of UAVs, there are several approaches that have been considered, such as leader-follower, virtual structure and behavior-based [1]. In Leader-Follower approach, one or some of the UAVs will be assigned as leader and others will be assigned as a follower. The followers are designed to track the position and orientation of leader with a predefined offset. The advantage of the leader-follower approach is the specifying the leader's motion could direct the group behavior [2].

A typical quadrotor consists of four Brushless Direct Current Motors (BLDCMs), four Electronic Speed Controllers (ESCs), four propellers, radio remote controller, body frame and the main is the flight controller board in the middle. Other than those basic components, Global Positioning System (GPS), camera, ultrasonic sensor, battery monitor and other sensor or gadget can be assembled on the quadrotor as additional equipment. There are two types of a frame configuration in quadrotor: '+' configuration and 'X' configuration. 'X' configuration is well known in the market due to the maneuverability and stability compare to '+' configuration. By referring to the configuration of frames, the '+' configuration is often commonly used for beginners due to the ease and intuitive to fly and easier to figure out the orientation of quadcopter when flying. However, as mentioned above, a research described that 'X' configuration is more stable than '+' configuration because of the distribution of rotor force during hover. 'X' configuration of quadrotor is chosen in this paper. The four BLDCMs mounted at the end of each arm of body frame with symmetrically, each arm is typically 90 degrees apart. Two diagonal BLDCMs rotate in clockwise (CW) and the other two diagonal BLDCMs rotate in counterclockwise (CCW) in order to create opposite force for staying balanced. The propellers also need to be installed according to the direction of the motors.
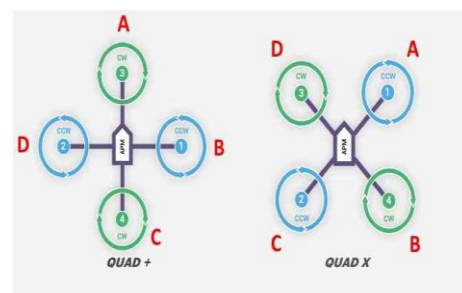

Figure 1: Frames Configuration of Quadrotor

II. Experimental Setup

This section will explain the detail of hardware used in this study. The hardware used is developed from scratch.

A. Quadrotor Construction

A typical quadrotor consists of the propulsion system, power source, telemetry, body frame, flight controller, gyro as the attitude sensor and Global Position System (GPS) as the position sensor. Figure-2 shows the detail of components used onboard.
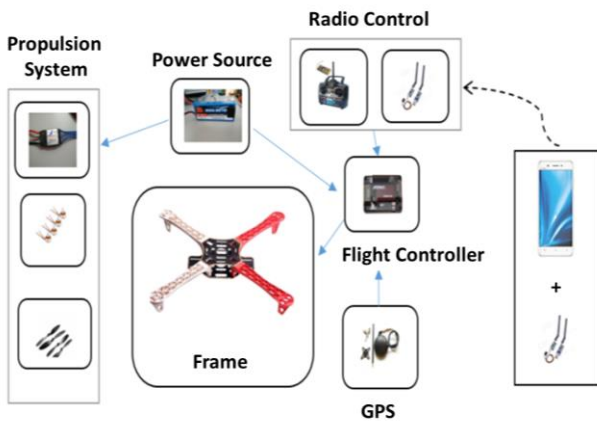

Figure 2: Quadrotor Components

The propulsion part of quadrotor involves three components which are Brushless Direct Current Motors (BLDCMs), propeller and Electronic Speed Controllers (ESCs). 920 KV BLDCMs had been chosen as the motor in this project since the 920 KV BLDCM is common in the market and easy to find the spare part. The maximum power of the BLDCMs is 165W and the maximum current draw is 15A. The weight of the BLDCMs is 52g for each. The ESCs chosen for this project is HobbyWing- xrotor 20A. ESCs are used to provide variable power to the BLDCMs. The higher power provides to the BLDCM, the high speed the BLDCM is, and vice-versa. Besides that, the chosen ESC also consist voltage cut-off features.

Lithium-ion Polymer battery, commonly known as LiPo battery is a rechargeable battery and it is commonly used in RC vehicle.

Frame F450 has been chosen as the frame of the quadrotor as it is compatible with most of the quadrotor and easy to assembly. This frame has integrated PCB plate that can direct solder the connection of Electronic Speed Controllers (ESCs) and power module. This enables the elimination of developing a power distribution board.

The radio controller used in this project is RadioLink T7F with seven channels and receiver is R7EH-s 7 Channels which is compatible with the controller.

Telemetry is also used in this project as the bridge for two ways communication between quadrotor and the Ground Control Station (GCS). This telemetry is very small in size and lighter weight resulting in the capable of installation on the quadrotor. The connection range between the pair of telemetry is approximately up to one mile (1.61 Km). One of the telemetries will be installed on the quadrotor and the other is connected to the GCS.

ArduPilot Mega (APM) 2.8 had been chosen as a flight controller in this project. APM is a professional IMU flight control that is based on Arduino Mega platform. APM is a full autopilot capable for way-point navigation, autonomous stabilization and also two ways telemetry. APM also provides eight RC channels with four serial ports. The most important thing is APM is open source software that updates constantly with latest and improved features. APM 2.8 had included six degrees of freedom (6 DOF) Inertial Measurement Unit (IMU), MPU 6000 which consists of three axis of the gyroscope and three axis of the accelerometer. Also, APM 2.8 consist high-performance barometric pressure sensor.

Global Positioning System (GPS) plays an important role in this project since the Leader-Follower approach will be based on the GPS navigation. There will be two GPS needed, one GPS in Android phone which acts as the leader and the other will be on the quadrotor as a follower. Since the Android phone has built-in onboard GPS, which could provide location or coordinates, the leader will use this GPS to generate the position information which will be sent to the follower.

GPS module installed on follower quadrotor is GY-NEO6MV2, also known as Ublox NEO-6M. The GPS receives data from the satellite by using the form of National Marine Electronics Association (NMEA).

B. Ground Control Station (GCS)

In this project, Mission Planner as an open source application is used as the Ground Control Station (GCS). Mission Planner is ready to use and developed to match with the flight controller, Ardupilot Mega (APM) 2.8.

Mission Planner is compatible with Windows only. In the assembly process, Mission Planner is used to configure all the setting and the calibration of APM 2.8. The calibrations include compass calibration, radio control (RC) calibration, accelerometer calibration, RC transmitter mode setup, motor arming speed, fail-safe setting and others.

Figure 3: Mission Planner

III. Quadrotor Dynamics and Modelling

This section presents the mathematical model of the quadrotor before designing the controller. As stated before, quadrotor in this project is using the 'X' configuration.

Figure 4 shows force distribution in a quadrotor. The arrow of F1, F2, F3 and F4 indicating the upward thrust force of each BLDCM whereas the '*m.g*' represents the gravitational force acting on a quadrotor. The thrust force is the vertical resultant forces which acting on all propellers whereas hub force is the horizontal force which acts on all propellers.

$$F_i = \frac{1}{2}\rho C_T \Omega_i^2 = b\Omega_i^2 \qquad (1)$$

$$H_i = \rho C_d \Omega_i^2 = d\Omega_i^2 \qquad (2)$$

$$F_{total} = \sum_{i=1}^{4} F_i \qquad (3)$$

where C_T is the thrust constant that relies on polar lift slope, the velocity through BLDCM, ratio of area surface, BLDCM disk area and geometric blade; ρ is air density; b is coefficient of thrust ; d is coefficient of drag; C_d represents drag constant and the Ω_i is the rotation speed of propeller.
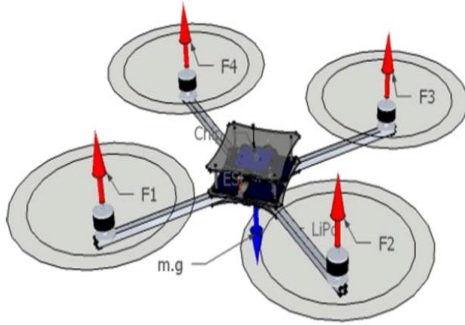

Figure 4: Force Distribution

Commonly, the control inputs of quadrotor are defined as u_1 , u_2 , u_3 and u_4 . Total force to control input is represented by u_1. Where, u_2 is roll torque, u_3 is pitch torque and u_4 is the yaw torque. τ_ϕ , τ_θ , τ_ψ are representing roll, pitch and yaw torque; l stands for the distance between each of BLCDM to the center of mass. $\dot{\phi}$, $\dot{\theta}$ and $\dot{\varphi}$ are roll, pitch and yaw angular body speed. Where, the $(-1)^{i+1}$ term is positive for the ith propeller if the propeller is spinning clockwise and negative if it is spinning counter clockwise. The total torque about the z-axis is given by the sum of all the torques from each propeller:

$$u_1 = \mathrm{b}F_{Total} = b\sum_{i=1}^{4} F_i$$
$$= b(\Omega_1^2 + \Omega_2^2 + \Omega_3^2 + \Omega_4^2) \qquad (4)$$

$$u_2 = \tau_\phi = bl(-F_2 + F_4) = bl(-\Omega_1^2 + \Omega_4^2) \qquad (5)$$

$$u_3 = \tau_\theta = bl(-F_1 + F_3) = bl(\Omega_1^2 - \Omega_3^2) \qquad (6)$$

$$u_4 = \tau_\psi = d\sum_{i=1}^{4} \Omega_i^2(-1)^{i+1} \qquad (7)$$

In order to simplify the model to comply with the real-time enforcement of the control loop, the hub forces and rolling moments are negligible but the drag coefficient, d and thrust coefficient, b should be a constant. The dynamic system of

quadrotor can be written in state space in term of $f(X,U)$ with the inputs vector, U and state vector, X as shown in Equation (8).

$$f(X,U) = \begin{bmatrix} \dot{x} \\ \ddot{x} \\ \dot{y} \\ \ddot{y} \\ \dot{z} \\ \ddot{z} \\ \dot{\phi} \\ \ddot{\phi} \\ \dot{\theta} \\ \ddot{\theta} \\ \dot{\psi} \\ \ddot{\psi} \end{bmatrix} = \begin{bmatrix} \dot{x} \\ \frac{(\cos\phi\sin\theta\cos\psi + \sin\phi\sin\psi)U_1}{m} \\ \dot{y} \\ \frac{(\cos\phi\sin\theta\sin\psi - \sin\phi\cos\psi)U_1}{m} \\ \dot{z} \\ -g + \frac{(\cos\phi\cos\theta)U_1}{m} \\ \dot{\phi} \\ \frac{U_2 + \dot{\theta}\dot{\psi}(I_{yy}-zz)}{I_{xx}} \\ \dot{\theta} \\ \frac{U_3 + \dot{\psi}\dot{\phi}(I_{zz}-I_{xx})}{I_{yy}} \\ \dot{\psi} \\ \frac{U_4 + \dot{\theta}\dot{\phi}(I_{xx}-I_{yy})}{I_{zz}} \end{bmatrix} \qquad (8)$$

where I_{xx}, I_{yy}, I_{zz} are body inertia of roll, pitch and yaw, respectively.

IV. CONTROL ARCHITECTURE

In quadrotor system, the attitude control which is involved in the roll, pitch and yaw angles are manipulated by the inner PID controller, while altitude control and position control is manipulated by the outer PID controller. Outer loop generates reference values for the inner loop. The attitude control had done in [3], so this paper discusses the position control and altitude control.
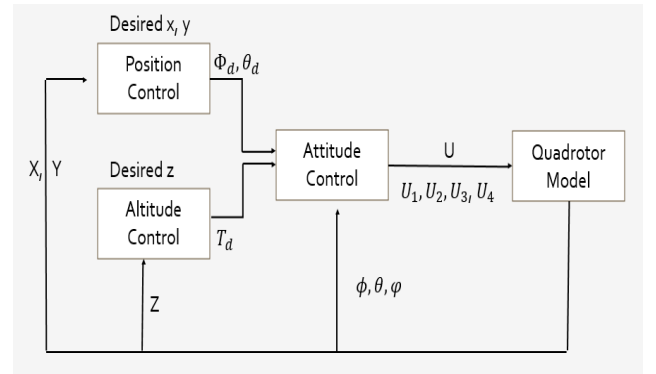

Figure 5: Control Architecture

A. Altitude Control

Altitude control is located in the outer loop, which is used to generate a thrust, T_d. This thrust lifts the quadrotor into the air, to the desired altitude. The equation of control law used for the altitude control is shown in Equation (9) and (10).

$$U_z = \ddot{z} = -g + \frac{u_1(\cos\phi\cos\theta)}{m} \qquad (9)$$

$$u_1 = \frac{m(g + PID_z)]}{\cos\phi\cos\theta} \qquad (10)$$

where

$$PID_z = K_{pz}(z(k)) + K_{iz} \sum_{i=0}^{k} (z(i)) \qquad (11)$$
$$+ K_{dz}(z_d(k))$$

where $z(k)$, $z_d(k)$ and $z(i)$ are deviation (error) of system, rate of change of error and integral error of system, respectively. Meanwhile, K_p, K_i and K_d are the gain values in term of proportional, integral and derivative, respectively.

B. Position Control

Position controller is also located in the outer loop, which is used to generate the desired roll and pitch angles. A PID controller is used in position control.

$$U_x = \ddot{x} = \frac{m}{U_1} PID_x \qquad (12)$$

$$U_y = \ddot{y} = \frac{m}{U_1} PID_y \qquad (13)$$

where

$$PID_x = K_{px}(x(k)) + K_{ix} \sum_{i=0}^{k} (x(i)) \qquad (14)$$
$$+ K_{dx}(x_d(k)))$$

$$PID_y = K_{py}(y(k)) + K_{iy} \sum_{i=0}^{n} (y(i)) \qquad (15)$$
$$+ K_{dy}(y_d(k))$$

where $x(k)$ is the deviation (error) of position on x-direction, $y(k)$ is the deviation (error) of position on y-direction, $x_d(k)$ is the rate of change of position error on x-direction, $y_d(k)$ is the rate of change of position error on y-direction, $x(i)$ is the integral position error on x-direction and $y(i)$ is the integral position error on y-direction. Additionally, K_p, K_i and K_d are the gain values in term of proportional, integral and derivative, respectively.

Roll (ϕ) and pitch (θ) angles are needed as to shift the quadrotor to the desired positions along x and y-axis. The output position control is fed as input for attitude control in the inner loop to generate the control inputs u_2 and u_3. The position control of x and y axis is based on the Equation (16) and (17) below:

$$U_x = \cos\phi \sin\theta \cos\psi + \sin\phi \sin\psi \qquad (16)$$

$$U_y = \cos\phi \sin\theta \sin\psi - \sin\phi \cos\psi \qquad (17)$$

By substituting Equation (16) and (17) into equation of $\ddot{x}$ and $\ddot{y}$ in Equation (12) and (13), yields:

$$\theta_d = \sin^{-1} \left[\frac{mPID_x}{U_1 \cos\phi_d} \right] \qquad (18)$$

$$\phi_d = -\sin^{-1} \left[\frac{mPID_y}{U_1} \right] \qquad (19)$$

C. Leader-Follower Approach

Most of the time, coordinated flight means a lot of several of vehicles are needed to maintain a specified formation shape [4][5]. Formation shape is the relative coordinate of the vehicle following the reference coordinate. In the simulation, a formation control was designed as the change in the horizontal displacement or altitude of follower respect to the reference altitude of leader.

$$Z_F = Z_L + Z_{constant} \qquad (20)$$

where Z_F will be the desired altitude of the follower quadrotor, Z_L denotes the altitude of leader and reference to follower, $Z_{constant}$ is represent the height between leader and follower. The control input for the follower is expressed by using Equation (21) and (22).

$$U_{xF} = \frac{m}{U_1} PID_{xF} \qquad (21)$$

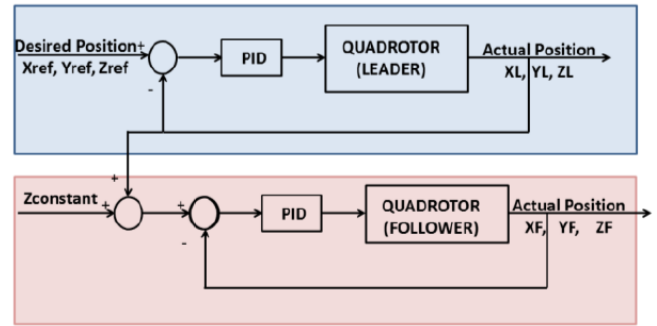$$U_{yF} = \frac{m}{U_1} PID_{yF} \qquad (22)$$

Figure 6: Control Architecture of Leader-Follower

In formation control, the follower's dynamical model is exactly the same as the leader. However, additional value in height ($Z_{constant}$) is added to maintain the quadrotors are in the safe position without colliding each other [6] [7].

V. RESULT AND DISCUSSION

The controller is designed in the Simulink by following the equation and architectural that is mentioned in section control architecture. However, before beginning the simulation, all the parameters used are collected from the assembled real hardware [10]. Table 1 shows the list of parameters of the developed quadrotor.

After tuning process, the PID gain values for each leader and follower quadrotor are shown in Table 2.

Table 1
Parameter of Quadrotor

Parameter	Value	Unit
m	0.9840	kg
l	0.1709	m
g	9.8100	ms^{-1}
J_R	3.7882e-06	Ns^{2}rad^{-1}
b	1.4865e-07	Ns^2
d	0.2223	Nms^2
I_{xx} , I_{yy}	0.0095	Ns^{2}rad^{-1}
I_{zz}	0.0186	Ns^{2}rad^{-1}

Table 2
PID Gain Values for Position and Altitude Control

	X_L	X_F	Y_L	Y_F	Z_L	Z_F
K_p	1.850	1.850	1.850	1.850	-2.625	-2.625
K_i	0.001	0.001	0.001	0.001	-0.153	-0.153
K_d	9.500	9.500	9.500	9.500	-9.996	-9.996

A. Step Response Analysis

A step input with magnitude one was fed to the whole system as the desired position x, y and desired altitude z to the quadrotor. The yaw input fix at zero radians in order to move the quadrotor without any yawing motion. The leader is moving to the desired position x, y, and z which are to 1 meter position each.

Figure 7 shows the performance of position x, y and altitude z by using PID gain values in Table 2. The time response analysis is summarized in Table 3. The result shows that the designed controller is capable enough to perform the leader-follower task. The overshoot percentage of position x and y are both 0 % for leader and the follower. Additionally, the overshoot percentage of leader and follower in the z-direction are 2.3% and 2.61%, respectively. The result also shows 0% steady state error among position control and altitude control in leader and follower.

B. Simulation of Circular Path

A circular path with 5 meter radius has been created and imported into the system. This path planning enables the leader to fly by following the desired path which is in a circular shape. As seen in Figure 8, the follower shows a good response to the leader by following the leader in a circular path as well. The PID values used in this task are the same with the PID values in step response. The time response of the system is shown in Figure 9. The time response analysis in term of overshoot percentage, settling time and rise time is not present here since the input is dynamically changing. The desired position is changing from time to time. However, the follower performance accuracy can be analyzed. This is done by observing the follower position relative to the leader position. The deviation of the follower is considered as the follower accuracy. As the result, the accuracy of the proposed system is 60, 80, 10 centimeter on x, y and z position, respectively. This result shows that the proposed method has good performance.

Table 3
Time Response Analysis for Step Input

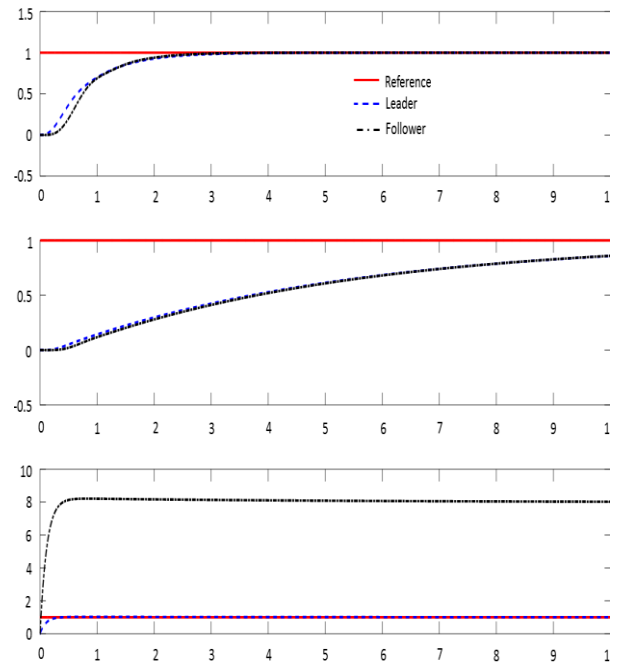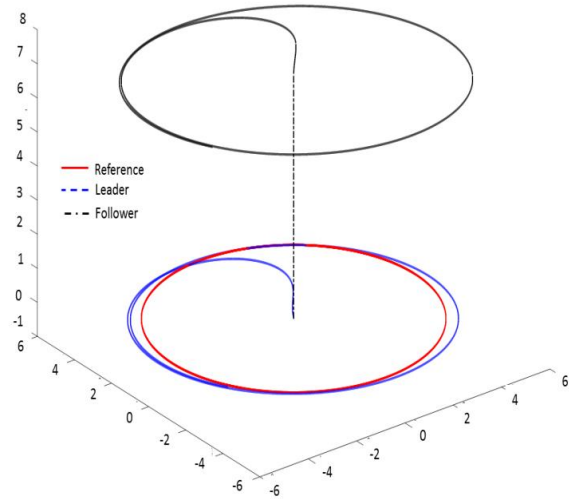|	Rise Time, T_r(s)	Settling Time, T_s(s)	Peak	Overshot Percentage, %	Steady state error, %
X_L	11.65	19.05	1.00	0.00	0.00
X_F	11.72	19.31	1.00	0.00	0.00
Y_L	11.65	19.05	1.00	0.00	0.00
Y_F	11.72	19.31	1.00	0.00	0.00
Z_L	0.20	0.36	1.023	2.30	0.00
Z_F	0.23	0.41	8.209	2.61	0.00

Figure 7: Position Control – Step Input

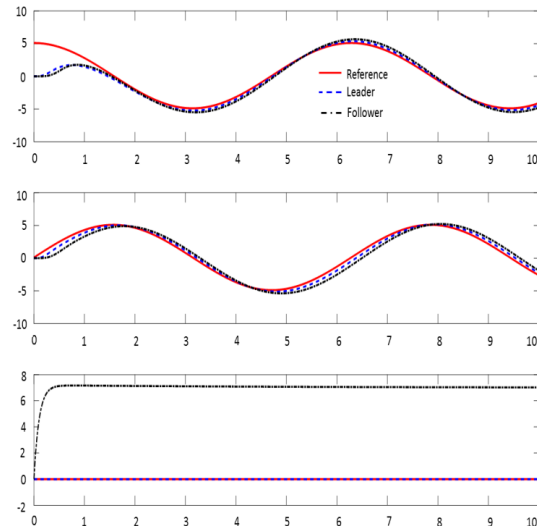Figure 8: 3D Position - Circular path

Figure 9: Position Control – Circular path

C. Hardware Performance

The designed controller and leader-follower algorithm are applied on the developed quadrotor. The time response analysis is then conducted. This analysis includes the analysis of rising time, settling time, peak and percentage of overshoot of the developed system.

The PID gain values used in the real flight is different from simulation since, in the real flight test, the environmental condition such as the wind speed is affecting the quadrotor. Additionally, in the real flight, a delay exists between Leader and Follower. This delay occurs due to the wireless communication between Leader and Follower. The PID gain values are summarized in Table 4.

Based on the real flight result shown in Figure 10 and Figure 11, the performance of the quadrotor in conducting leader-follower task is good. This can be seen from the figures that follower (dashed line) is following the leader (solid line). The detail of time response is summarized in Table 5. The overshoot percentage for x, y and z position of the follower are about 7%, 0% and 0%, respectively.
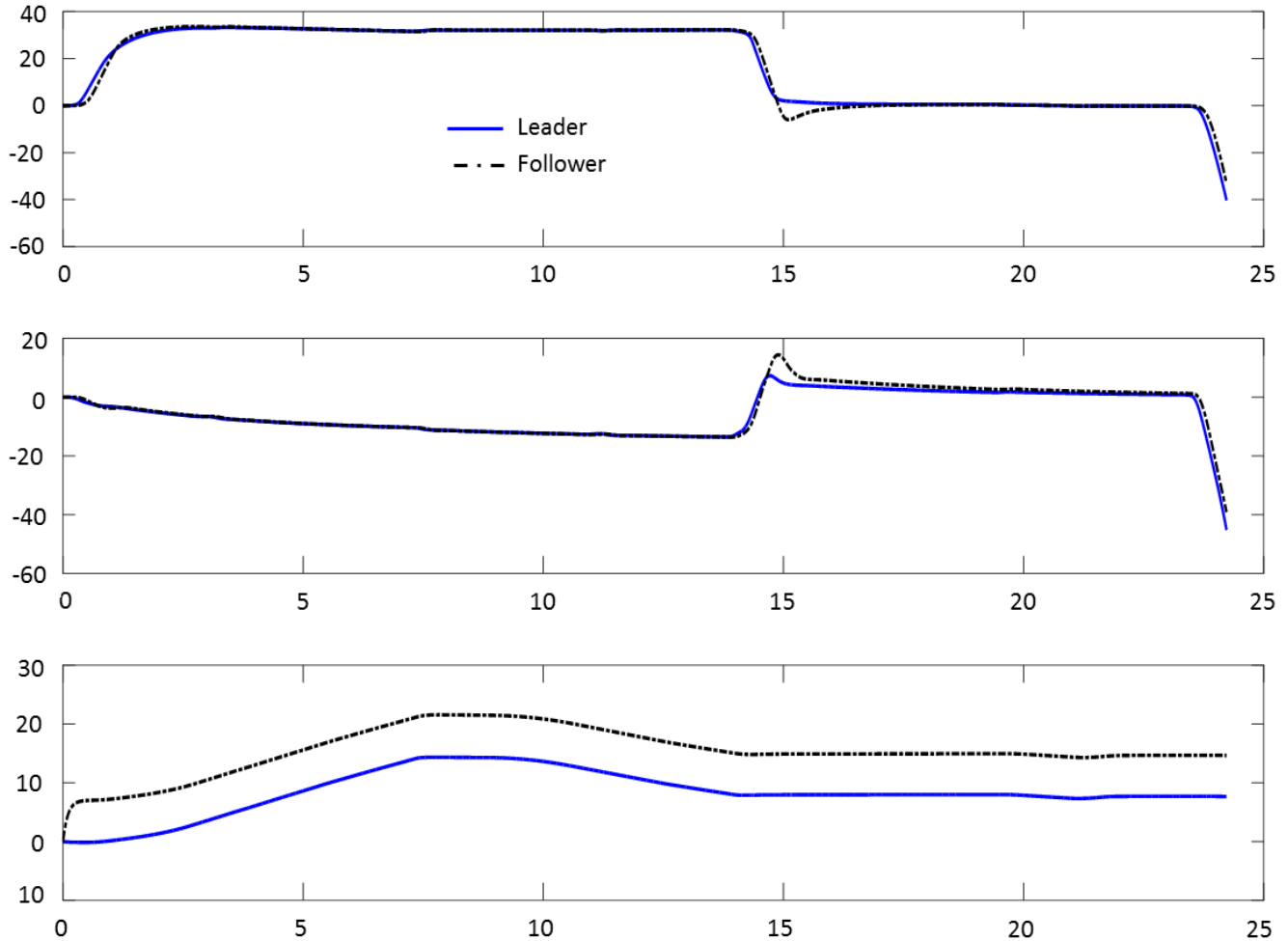

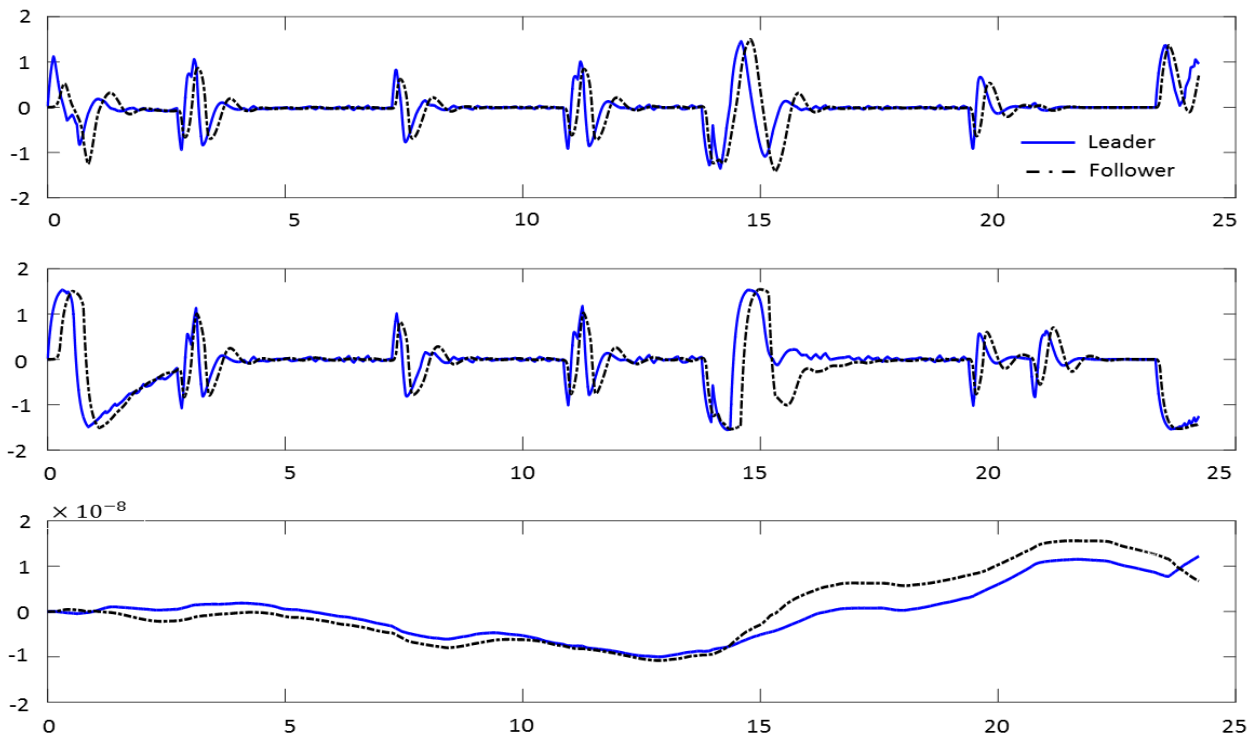Figure 10: Quadrotor Position – Hardware Implementation

Figure 11: Quadrotor Attitude – Hardware Implementation

Table 4
PID Gain Values for Hardware Implementation

	Roll	Pitch	Yaw
K_p	0.2493	0.2496	0.17
K_i	0.2496	0.2496	0.02
K_d	0.003	0.0055	0.003

Table 5
Time Response Analysis of Real Flight

Position	Rise Time, $T_r (s)$	Settling Time, T_s (s)	Peak	Overshot Percentage, %
$X_{Follower}$	8.5	10.22	0.07134	7.134
$Y_{Follower}$	7.9	10.90	35.2800	0.000
$Z_{Follower}$	17.7	19.45	8.0000	0.000

VI. CONCLUSION

As a conclusion, a quadrotor had been developed from scratch. This quadrotor is able to follow a leader with high accuracy. The position control and altitude control of quadrotor are designed in the simulation by using Matlab Simulink. PID controller is implemented on a quadrotor. From the real flight experiment, it is shown that the PID controller has good performance to maintain the quadrotor following the leader with an average of 7% overshoot and the steady-state error is 0%.

The experiment was conducted in a soccer field with the distance between leader and follower is maintained to be less than 500 meters. Additionally, both leader and follower were maintained to be close enough to the Ground Station in order to track their position. As future works, sensor network needs to be considered in the application so that the formation control between leader and follower can be expanded into a longer distance. Therefore, broader applications such as forest monitoring, coastal area monitoring can be conducted.

REFERENCES

[1] Qin, W., Liu, Z., & Chen, Z, "Formation control for nonlinear multi-agent systems with linear extended state observer", *IEEE/CAA Journal of Automatica Sinica*, 1(2), pp: 171–179, 2014.

[2] Abbas, R., & Wu, Q., "Improved Leader-Follower Formation controller for multiple Quadrotors based AFSA", *TELKOMNIKA (Telecommunication Computing Electronics and Control)*, 13(1), pp: 85–92, 2015.

[3] Nurul Amirah, I., Nor Liyana, O., Zain, Z. M., Dwi, P., & Luhur, B., "Attitude control of a quadrotor", *ARPN Journal of Engineering and Applied Science*, 10(22), pp: 17206-17211, 2015.

[4] Tonetti, S., Hehn, M., Lupashin, S., & D'Andrea, R., "Distributed control of antenna array with formation of UAVs", *IFAC Proceedings Volumes (IFAC-PapersOnline)*, *18*(PART 1), pp: 7848–7853, 2011.

[5] Franchi, A., Masone, C., Grabe, V., Ryll, M., Bülthoff, H. H., & Giordano, P. R., "Modeling and Control of UAV Bearing Formations with Bilateral High-level Steering", *The International Journal of Robotics Research*, 31(12), pp: 1504–1525, 2012.

[6] Cheng, H., Chen, Y., Li, X., & Shing, W. W., "Autonomous takeoff, tracking and landing of a UAV on a moving UGV using onboard monocular vision", *Chinese Control Conference, CCC,* pp: 5895–5901, 2013.

[7] Ghamry, K. A., Dong, Y., Kamel, M. A., & Zhang, Y., "Real-time autonomous take-off, tracking and landing of UAV on a moving UGV platform", *24th Mediterranean Conference on Control and Automation, MED 2016*, pp: 1236–1241, 2016.

[8] Cheng, H., Chen, Y., & Wong, W. S., "Trajectory tracking and formation flight of autonomous UAVs in GPS-denied environments using onboard sensing", *2014 IEEE Chinese Guidance, Navigation and Control Conference, CGNCC 2014*, pp: 2639–2645, 2015.

[9] Turpin, M., Michael, N., & Kumar, V., "Trajectory design and control for aggressive formation flight with quadrotors", *Autonomous Robots*, 33(1–2), pp: 143–156, 2012.

[10] Tamami, N., Pitowarno, E., & Astawa, I. G. P., "Proportional Derivative Active Force Control for "X Configuration Quadcopter", *Journal of Mechatronics, Electrical Power, and Vehicular Technology*, 5(2), pp: 67-74, 2014.